bioRxiv preprint doi: https://doi.org/10.1101/138651; this version posted May 17, 2017. The copyright holder for this preprint (which was not certified by peer review) is the author/funder, who has granted bioRxiv a license to display the preprint in perpetuity. It is made available under aCC-BY-NC-ND 4.0 International license.



# Hydrogen isotope composition of *Thermoanaerobacterium saccharolyticum* lipids: comparing wild type to a *nfn*-transhydrogenase mutant

William D. Leavitt[a,b,c,*], Sean Jean-Loup Murphy[d,e], Lee R. Lynd[c,d,e], Alexander S. Bradley[a,f,*]

[a] Department of Earth and Planetary Sciences, Washington University in St. Louis, Saint Louis, MO 63130 USA
[b] Department of Earth Sciences, Dartmouth College, Hanover, NH 03755 USA
[c] Department of Biological Sciences, Dartmouth College, Hanover, NH 03755 USA
[d] Thayer School of Engineering, Dartmouth College, Hanover, NH 03755 USA
[e] BioEnergy Science Center, Oak Ridge National Laboratory, Oak Ridge TN 37830, USA
[f] Division of Biology and Biomedical Sciences, Washington University in St. Louis, Saint Louis, MO 63130 USA

*Correspondence authors e-mail addresses: william.d.leavitt@dartmouth.edu (W.D. Leavitt, abradley@eps.wustl.edu (A.S. Bradley).

## *Abstract*

**The $^{2}H/^{1}H$ ratio in microbial fatty acids can record information about the energy metabolism of microbes and about the isotopic composition of environmental water. However, the mechanisms involved in the fractionation of hydrogen isotopes between water and lipid are not fully resolved. We provide data aimed at understanding this fractionation in the Gram-positive obligately thermophilic anaerobe, *Thermoanaerobacterium saccharolyticum,* by comparing a wild-type strain to a deletion mutant in which the *nfnAB* genes encoding electron-bifurcating transhydrogenase have been removed. The wild-type strain showed faster growth rates and larger overall fractionation ($^{2}\varepsilon_{total}$ -319±4 ‰) than the mutant strain ($^{2}\varepsilon_{total}$ -298±4 ‰). The overall trend in growth rate and fractionation, along with the isotopic ordering of individual lipids, is consistent**

bioRxiv preprint doi: https://doi.org/10.1101/138651; this version posted May 17, 2017. The copyright holder for this preprint (which was not certified by peer review) is the author/funder, who has granted bioRxiv a license to display the preprint in perpetuity. It is made available under aCC-BY-NC-ND 4.0 International license.



**with results reported for the Gram-negative sulfate reducer, *Desulfovibrio alaskensis* G20.**

## 1. Introduction

The fractionation of hydrogen isotopes between environmental water and microbial biomass lipids correlates with central energy metabolism in many aerobic and some anaerobic bacteria (Dawson et al., 2015; Heinzelmann et al., 2015; Osburn et al., 2016; Zhang et al., 2009). The correlation has been inferred to relate to the mechanisms controlling the production of intracellular electron carriers such as NADPH and NADH. In some anaerobic bacteria the pattern of fractionation is more complicated, and does not strongly correlate with central carbon metabolism (Dawson et al., 2015; Leavitt et al., 2016; Osburn et al., 2016). One potential explanation for this complexity relates to the importance of flavin-based electron bifurcation by transhydrogenase in anaerobes (Demmer et al., 2015). These enzymes may impose a large isotope effect, which could overprint signals that relate primarily to carbon metabolism. Examination of transhydrogenase mutants in *Desulfovibrio alaskensis* G20 showed that on substrates such as malate and fumarate, perturbed transhydrogenase significantly affected the •$^{2}$H values of lipids (Leavitt et al., 2016).

A more complete understanding of factors that impact •$^{2}H_{lipid}$ might be achieved by examination of microbial strains with different strategies for NAD(P)H regulation. The production of NADPH is critical for lipid

bioRxiv preprint doi: https://doi.org/10.1101/138651; this version posted May 17, 2017. The copyright holder for this preprint (which was not certified by peer review) is the author/funder, who has granted bioRxiv a license to display the preprint in perpetuity. It is made available under aCC-BY-NC-ND 4.0 International license.



biosynthesis. This cellular metabolite can derive from multiple sources, including reactions of central carbon metabolism, production from NADH via transhydrogenase, and production from NADH by NAD kinases. Three types of NAD kinases have been described (Kawai and Murata, 2008), with subcategories found in (i) Gram positive (+) bacteria and archaea, (ii) eukaryotes, and (iii) Gram negative (-) bacteria. In Gram(+) bacteria such as *Thermoanaerobacterium saccharolyticum*, NAD kinase can use ATP or polyphosphate as a P source. Few data exist on hydrogen isotopic fractionation in Gram(+) bacteria (Valentine et al., 2004). In this study, we apply a molecular genetic approach to examine hydrogen isotopic fractionation in a model Gram(+) organism, *T. saccharolyticum*. We compare the wild-type strain to a transhydrogenase-deficient mutant to determine phenotypic effects on growth rate, lipid profile, and magnitude of hydrogen isotopic fractionation between medium water and lipid. Our findings show patterns similar to those observed for *D. alaskensis* G20 (Leavitt et al., 2016).

## 2. **Methods**

*T. saccharolyticum* strain JW/SL-YS485 (wild type) was cultivated in parallel with a recently reported NfnAB transhydrogenase-deficient mutant (Lo et al., 2015), strain LL1144 (•*nfnAB*::Kan$^{r}$). Triplicate cultures of each were grown at 55 °C in 150 ml glass bottles with a 50 ml working volume in MTC defined medium on 5 g/l cellobiose, as detailed in the Supplement.

bioRxiv preprint doi: https://doi.org/10.1101/138651; this version posted May 17, 2017. The copyright holder for this preprint (which was not certified by peer review) is the author/funder, who has granted bioRxiv a license to display the preprint in perpetuity. It is made available under aCC-BY-NC-ND 4.0 International license.



Cells were harvested at early stationary phase by way of centrifugation and were lyophilized. Lipid extraction, derivatization and analysis protocols were identical to those reported by Leavitt et al. (2016). Lipid retention times and peak areas were determined by gas chromatography-mass spectrometry (GC-MS), the •$^2$H values of lipids measured by GC isotope ratio mass spectrometry (GC-IRMS) and the •$^2$H of water samples by duel-inlet IRMS and cavity ring-down spectroscopy (CRDS), following Leavitt et al. (2016). The •$^2$H values are reported relative to V-SMOW (Vienna Standard Mean Ocean Water) and fractionation is reported as apparent fractionation between medium water and lipid from the equation: $^2$•$_{lipid/water}$ = ($^2$•$_{lipid/water}$ -1), where • = [(•$^2$H$_{lipid}$ + 1000)/(•$^2$H$_{water}$ + 1000)]. Each lipid from each culture sample (representing each individual biological triplicate) was measured 14 to 20 times.

## 3. Results

The doubling time of the wild-type strain was 0.33 ± 0.10 h$^{-1}$, compared vs. a slower growth rate of 0.10 ± 0.01 h$^{-1}$ for the •*nfnAB* strain (Fig. 1). The wild-type strain demonstrated a longer lag phase, perhaps because it was inoculated at a lower initial cell density than the mutant. The maximum optical density (OD) for the wild-type was nearly 3-times that of the mutant, with average final OD$_{600}$: wild-type = 1.04 (±0.03) vs. •*nfnAB* = 0.37 (±0.01), representing biological triplicates of each strain (Fig. 1).

bioRxiv preprint doi: https://doi.org/10.1101/138651; this version posted May 17, 2017. The copyright holder for this preprint (which was not certified by peer review) is the author/funder, who has granted bioRxiv a license to display the preprint in perpetuity. It is made available under aCC-BY-NC-ND 4.0 International license.



The lipid profile of *T. saccharolyticum* was similar to what has been previously reported from this genus (Jung and Zeikus, 1994). The strain produced abundant *n*-$C_{16}$ fatty acids (FA) along with branched *iso-* and *anteiso-* $C_{15}$ and $C_{17}$ FA. Smaller amounts of *n*-$C_{14}$ FA were detected, along with a long-chain dicarboxylic acid. The mass spectrum of the latter was consistent with one reported from *T. ethanolicus* (Jung and Zeikus, 1994). The wild-type had elevated concentrations of the *iso-* FA relative to the mutant, but the lipid profiles were otherwise similar (Fig. 2).

The mass-weighted average hydrogen isotopic fractionation between water and lipid ($^{2}\bullet_{total}$) was greater for the wild type (-319±4 ‰) than for •*nfnAB* (-298±4 ‰). The fractionation ($^{2}\bullet$) for each individual lipid was also greater in the wild type than in the mutant (Fig. 3). The isotopic ordering of individual lipids ($^{2}\bullet_{lipid/water}$) was similar for both strains, with *anteiso-* lipids depleted relative to *iso-* and straight chain FA. The relative ordering from most depleted lipid (*anteiso*-$C_{15:0}$) to most enriched (iso-$C_{17:0}$), was nearly identical for both wild-type and mutant (Fig. 3).

## 4. Discussion

Observation of the $^{2}\bullet_{lipid/water}$ and $^{2}\bullet_{total}$ in wild-type and *nfnAB* transhydrogenase mutant strains of *D. alaskensis* G20 revealed that faster growing strains were more depleted in $^{2}H$ than the slower strains (Leavitt et al., 2016). *T. saccharolyticum* also showed similar relationships between growth rate and fractionation. Whether this pattern can be attributed to a

bioRxiv preprint doi: https://doi.org/10.1101/138651; this version posted May 17, 2017. The copyright holder for this preprint (which was not certified by peer review) is the author/funder, who has granted bioRxiv a license to display the preprint in perpetuity. It is made available under aCC-BY-NC-ND 4.0 International license.



126 similar role for the influence of transhydrogenase on •$^{2}H_{lipid}$, a consistent
127 relationship with growth rate and •$^{2}H_{lipid}$, or a more nuanced relationship
128 due to changes in both NfnAB activity and growth rate, remains unresolved.
129 Deconvoluting these possibilities will require steady-state experiments with
130 both strains cultured in parallel at a fixed growth rate. Growth rate effects
131 have been observed on •$^{2}H_{lipid}$ in haptophyte algae (Sachs and Kawka, 2015;
132 Schouten et al., 2006), and chemostat experiments have been used to
133 understand fractionation as a function of rate in other isotope systems
134 (Leavitt et al. 2013).

135 Another commonality between *T. saccharolyticum* and *D. alaskensis*
136 is the $^{2}H$ depletion in the *anteiso-* FA relative to the other FA (Fig. 3).
137 Leavitt et al. (2016) suggested that this depletion might originate in the
138 biosynthesis of *anteiso-* FA from 2-methylbutyryl-CoA derived from
139 isoleucine. This explanation could also be invoked for *T. saccharolyticum*,
140 and compound-specific •$^{2}H$ measurements of amino acids might provide
141 valuable constraints on the isotopic ordering among lipids. A recent study of
142 the H isotopic compositions of individual amino acids in *Escherichia coli*
143 grown on glucose and tryptone showed that isoleucine was depleted in $^{2}H$
144 relative to leucine by ca. 100‰ (Fogel et al., 2016).

145

146 **5. Conclusions**

147 Deletion of the electron-bifurcating transhydrogenase, NfnAB, slows
148 growth rate and decreases the magnitude of $^{2}•_{lipid/water}$ and $^{2}•_{total}$ when *T.*
149 *saccharolyticum* is grown on a defined medium in batch culture. The

bioRxiv preprint doi: https://doi.org/10.1101/138651; this version posted May 17, 2017. The copyright holder for this preprint (which was not certified by peer review) is the author/funder, who has granted bioRxiv a license to display the preprint in perpetuity. It is made available under aCC-BY-NC-ND 4.0 International license.



150 relative ordering of $^{2}\epsilon_{lipid/water}$ is similar in both strains. These patterns of
151 fractionation and isotopic ordering are similar to recent observations of the
152 heterotrophic sulfate reducer *D. alaskensis* G20. The consistency of results
153 across these taxa supports a role for NfnAB in determining the H isotopic
154 composition of lipids in obligate anaerobes. However, to better constrain
155 these observations, and isolate the effect of growth rate, continuous culture
156 (chemostat) experiments are necessary. Similar work with a broader array
157 of transhydrogenase-containing microbes would be helpful, including
158 organisms utilizing families of transhydrogenases other than NfnAB-class.
159 Such experiments can place further constrains on the mechanism(s) of lipid
160 H-isotopic fractionation.
161
162 **6. Supplementary information**
163 All supplemental methods and data are archived at:
164 10.6084/m9.figshare.4598224.
165
166 ***Acknowledgments***
167 We thank K. Grice and J. Maxwell for editorial handling and an
168 anonymous reviewer whose comments helped improve the manuscript. We
169 are grateful to M. Seuss (Washington University) for assistance with lipid
170 analysis, X. Feng (Dartmouth College) and M. Osburn (Northwestern
171 University) for water H-isotope analysis and the Lynd lab (Dartmouth
172 College) for assistance with growth experiments. Funding was provided by
173 U.S. NASA Exobiology grant 13-EXO13-0082 (A.S.B., W.D.L.), and the

bioRxiv preprint doi: https://doi.org/10.1101/138651; this version posted May 17, 2017. The copyright holder for this preprint (which was not certified by peer review) is the author/funder, who has granted bioRxiv a license to display the preprint in perpetuity. It is made available under aCC-BY-NC-ND 4.0 International license.



174 Fossett Postdoctoral Fellowship from Washington University in St. Louis
175 (W.D.L.). The BioEnergy Science Center is supported by the Office of
176 Biological and Environmental Research in the U.S. Department of Energy
177 Office of Science. The manuscript has been authored in part by Dartmouth
178 College under Contract no. DE-AC05-00OR22725 with the U.S. Department
179 of Energy.
180

181 ***References***

182 Dawson, K.S., Osburn, M.R., Sessions, A.L., Orphan, V.J., 2015. Metabolic
183 associations with archaea drive shifts in hydrogen isotope fractionation
184 in sulfate-reducing bacterial lipids in cocultures and methane seeps.
185 Geobiology 13, 462–477. doi:10.1111/gbi.12140
186 Demmer, J.K., Huang, H., Wang, S., Demmer, U., Thauer, R.K., Ermler, U.,
187 2015. Insights into Flavin-based Electron Bifurcation via the NADH-
188 dependent Reduced Ferredoxin:NADP Oxidoreductase Structure. J.
189 Biol. Chem. 290, 21985–21995. doi:10.1074/jbc.M115.656520
190 Fogel, M.L., Griffin, P.L., Newsome, S.D., 2016. Hydrogen isotopes in
191 individual amino acids reflect differentiated pools of hydrogen from food
192 and water in *Escherichia coli*. Proc. Natl. Acad. Sci. 201525703.
193 doi:10.1073/pnas.1525703113
194 Heinzelmann, S.M., Villanueva, L., Sinke-Schoen, D., Sinninghe Damsté,
195 J.S., Schouten, S., van der Meer, M.T.J., 2015. Impact of metabolism
196 and growth phase on the hydrogen isotopic composition of microbial
197 fatty acids. Front. Microbiol. 6, 1–11. doi:10.3389/fmicb.2015.00408

bioRxiv preprint doi: https://doi.org/10.1101/138651; this version posted May 17, 2017. The copyright holder for this preprint (which was not certified by peer review) is the author/funder, who has granted bioRxiv a license to display the preprint in perpetuity. It is made available under aCC-BY-NC-ND 4.0 International license.



198 Jung, S., Zeikus, J.G., 1994. A new family of very long chain a,o-dicarboxylic
199 acids is a major structural fatty acyl component of the membrane lipids
200 of Thermoanaerobacter ethanolicus 39E. J. Lipid Res. 35, 1057–1065.
201 Kawai, S., Murata, K., 2008. Structure and function of NAD kinase and
202 NADP phosphatase: key enzymes that regulate the intracellular
203 balance of NAD(H) and NADP(H). Biosci. Biotechnol. Biochem. 72, 919–
204 930. doi:10.1271/bbb.70738
205 Leavitt, W.D., Flynn, T.M., Suess, M.K., Bradley, A.S., 2016.
206 Transhydrogenase and growth substrate influence lipid hydrogen
207 isotope ratios in Desulfovibrio alaskensis G20. Front. Microbiol. 7.
208 doi:10.3389/fmicb.2016.00918
209 Lo, J., Zheng, T., Olson, D.G., Ruppertsberger, N., Tripathi, S. a., Guss,
210 A.M., Lynd, L.R., 2015. Deletion of *nfnAB* in *Thermoanaerobacterium*
211 *saccharolyticum* and its effect on metabolism. J. Bacteriol. 197,
212 JB.00347-15. doi:10.1128/JB.00347-15
213 Osburn, M.R., Dawson, K.S., Fogel, M.L., Sessions, A.L., 2016.
214 Fractionation of hydrogen isotopes by sulfate- and nitrate-reducing
215 bacteria. Front. Microbiol. 7, 1166.
216 Sachs, J.P., Kawka, O.E., 2015. The influence of growth rate on 2H/1H
217 fractionation in continuous cultures of the coccolithophorid Emiliania
218 huxleyi and the diatom Thalassiosira pseudonana. PLoS One 10,
219 e0141643. doi:10.1371/journal.pone.0141643
220 Schouten, S., Ossebaar, J., Schreiber, K., Kienhui, s M.V.M., Langer, G.,

bioRxiv preprint doi: https://doi.org/10.1101/138651; this version posted May 17, 2017. The copyright holder for this preprint (which was not certified by peer review) is the author/funder, who has granted bioRxiv a license to display the preprint in perpetuity. It is made available under aCC-BY-NC-ND 4.0 International license.



221 Benthien, A., Bijma, J., 2006. The effect of temperature, salinity and
222 growth rate on the stable hydrogen isotopic composition of long chain
223 alkenones produced by Emiliania huxleyi and Gephyrocapsa oceanica.
224 Biogeosciences 3, 113–119. doi:10.5194/bg-3-113-2006
225 Valentine, D.L., Sessions, A.L., Tyler, S.C., Chidthaisong, A., 2004.
226 Hydrogen isotope fractionation during H2/CO2 acetogenesis: hydrogen
227 utilization efficiency and the origin of lipid-bound hydrogen. Geobiology
228 2, 179–188. doi:doi:10.1111/j.1472-4677.2004.00030.x
229 Zhang, X., Gillespie, A.L., Sessions, A.L., 2009. Large D/H variations in
230 bacterial lipids reflect central metabolic pathways. Proc. Natl. Acad.
231 Sci. U. S. A. 106, 12580–6. doi:10.1073/pnas.0903030106
232
233

bioRxiv preprint doi: https://doi.org/10.1101/138651; this version posted May 17, 2017. The copyright holder for this preprint (which was not certified by peer review) is the author/funder, who has granted bioRxiv a license to display the preprint in perpetuity. It is made available under aCC-BY-NC-ND 4.0 International license.



234 **Figure 1.**

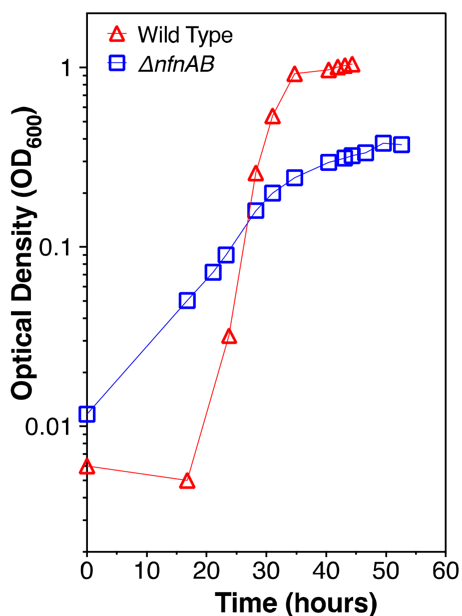


235

236 Fig. 1. Growth curves and
237 calculated doubling times for wild-
238 type and mutant (avg. of triplicate
239 growth experiments).
240

241 **Figure 2.**

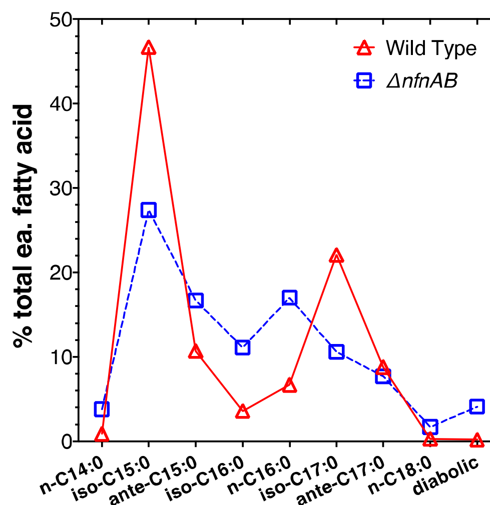


Fig. 2. Lipid abundance profiles for
244 wild type and mutant (avg. of
245 triplicate growth experiments).
246
247
248
249

bioRxiv preprint doi: https://doi.org/10.1101/138651; this version posted May 17, 2017. The copyright holder for this preprint (which was not certified by peer review) is the author/funder, who has granted bioRxiv a license to display the preprint in perpetuity. It is made available under aCC-BY-NC-ND 4.0 International license.



250 **Figure 3.**

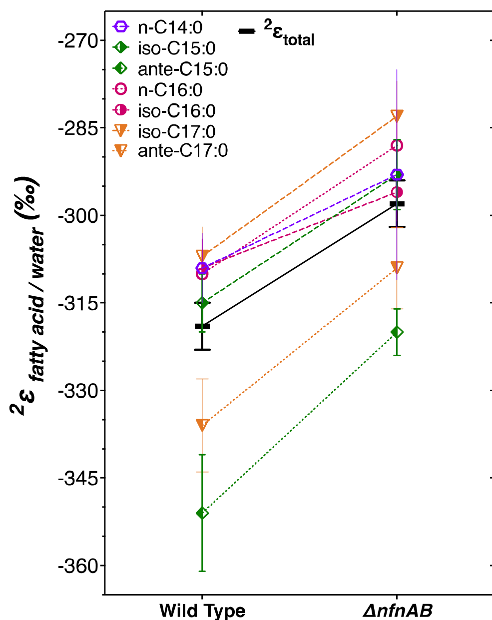


251
252 Fig. 3. H isotope fractionations
253 between FA and water. Black
254 horizontal bar, weighted mean for
255 each strain. Vertical bars, standard
256 mean error (SME) for all biological
257 (N = 3) and technical replicates (n =
258 14 to 20).

259
260

261 **Figure 4.**

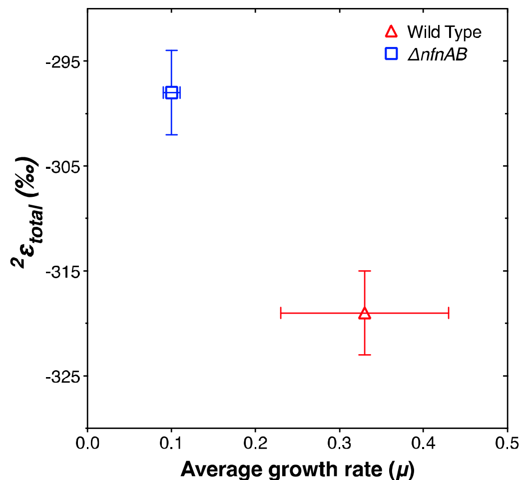


Fig. 4. Weighted H- isotopic fractionation between FA and water
265 for each strain vs. average doubling
266 time.
267